Scales of Metal Fatigue Limit

A. A. Shanyavskiy[1]* and A. P. Soldatenkov[1]

[1] *Aviation Register of the Russian Federation, Sheremetyevo Airport, Moscow region, 141426 Russia*
* e-mail: 106otdel@mail.ru

Abstract—The paper analyzes the scale hierarchy of transitions from very high to high and low cycle fatigue which are taken as fatigue limit according to the Wöhler concept. The analysis shows that the life distribution in the transition range 10^6–10^8 cycles is multimodal. From relations between the fatigue limit σ_{-1} and mechanical characteristics σ_U and $\sigma_{0.2}$ in aircraft materials based on Fe, Al, Mg, Ti, and Cu it follows that σ_{-1} depends on σ_U and $\sigma_{0.2}$ and the ratio $\sigma_{-1}/\sigma_{0.2}$ depends on $\sigma_{0.2}/\sigma_U$. As $\sigma_{-1}/\sigma_{0.2}$ increases, the complete diagram of three fatigue scales degrades. The transition from very high to low cycle fatigue goes without high cycle fatigue at $\sigma_{-1}/\sigma_{0.2} \geq 1$.

Keywords: fatigue limit, mechanical characteristics, aircraft structural materials, scales

1. INTRODUCTION

Conventionally, the fatigue failure of metals is described by the Wöhler curve with the stress amplitude σ_a related to the number of cycles to failure N_f as [1]

$$N_f \sigma_a^m = \text{const.} \qquad (1)$$

The exponent m, being a material characteristic, depends on the fatigue regime: low cycle fatigue (LCF) at up to 10^5 cycles and high cycle fatigue (HCF) at more than 10^5 [1].

The upper boundary of high cycle fatigue is 10^8 cycles, and the stress without failure determined in a material at 10^7–10^8 is taken as its fatigue limit: σ_{-1} for symmetric cycling [2].

However, such an interpretation of metal fatigue is inadequate as failure at stresses lower than σ_{-1} may occur in the range $>10^8$–10^{10} cycles [3]. This range is associated with subsurface crack nucleation and is termed very high cycle fatigue (VHCF) [4–7].

The fatigue life of a material, as its response to external action, depends on the material type and strength. Hence, different materials at the same external stress can differ in durability such that their life can lie in any of the above-mentioned three regimes and their fatigue limit σ_{-1} can fall on any boundary of the three.

From synergetic principles and evolution of scales in open systems, the fatigue life of metals can be represented as a bifurcation diagram (Fig. 1) in terms of equivalent stress or strain energy density accumulated per unit metal volume, e.g., per grain [8]. In the diagram, the transitions from stage to stage are bifurcation regions in which either of two respective failure mechanisms at the same stress is possible with a certain probability. Of significance here is that such bifurcation regions provide two different ways of energy absorption, each dominating on its own previous or next scale, and this provides a bimodal life distribution in these regions.

In terms of equivalent stress and strain energy density, the behavior of metals under cyclic loads can be described by a cascade of fatigue curves of the form

$$N_f \sigma_e^{m_i} = C_i, \qquad (2)$$

where the lower index $i = 1, 2, 3$ differentiates three scales identified with three fatigue regimes: 1—micro- or nanoscale with very high cycle fatigue, 2—mesoscale with high cycle fatigue, and 3—macroscale with low cycle fatigue.

Noteworthy in this connection is a fatigue diagram suggested by Mughrabi [9]. Being based on the Wöhler concept, the diagram explains the transition from low to very high cycle fatigue, i.e., from surface to subsurface fracture in order of decreasing stress, with a single stress level assigned to high cycle fatigue and taken as fatigue limit (Fig. 2). For damage accumulation via surface crack nucleation in intense slip bands, a relation is proposed between the slip band density
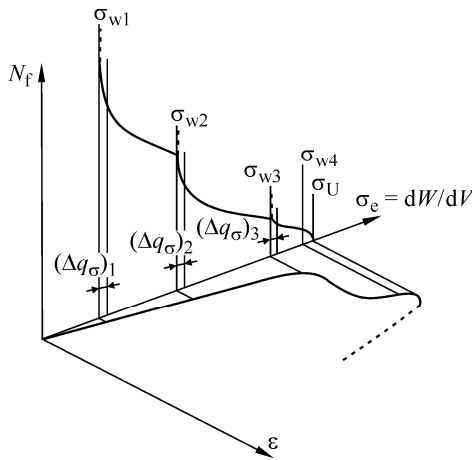
Fig. 1. Bifurcation diagram of metal fatigue N_f–σ_e with tension σ_e–ε in terms of equivalent stress σ_e or strain energy density dW/dV with bifurcation regions $(\Delta q_\sigma)_i$ for transitions to micro- or nanoscale (σ_{w1}–σ_{w2}), mesoscale (σ_{w2}–σ_{w3}), and macroscale (σ_{w3}–σ_{w4}).

Fig. 2. Mughrabi diagram, according to Wöhler concept, for transition from low to very high cycle fatigue [9].

$\overline{p}$ and the number of cycles to failure of up to 10^6 for copper [9].

In physical mesomechanics, the evolution of plastic deformation is considered as a sequence of processes from the micro- or nano- to the macroscale via the mesoscale [10]. In this context, the accumulation of damages on the macroscale in low cycle fatigue should be driven not only by intense sliding under developed plastic strains but also by vortex flows up to grain rotations and knife boundary formation. These processes, being final in the scale hierarchy, are inoperative on the mesoscale when high cycle fatigue occurs in metals.

If we put one scale for metal fatigue up to its very high cycle fatigue regime, we will have a contradiction with the linear cumulative damage rule in lifetime models of unsteadily loaded parts [11, 12]. The rise of residual strains associated with nonlinear damage accumulation excludes the use of this rule though it holds in many practical cases, e.g., in estimating the lifetime of aerostructures.

Moreover, metal parts in most cases operate with different types of joints (rivets, bolts, welds, etc.) and may suffer from residual strains only at overloads, i.e., at loads other than rated or recommended. For example, such strains can be found neither in compressor disks of aircraft gas turbine engines after 6000 flights [13] nor in their turbine disks after 2000 flights [14]. The rise of residual strains changes the geometry and conditions of loading such that the blades of an engine touch its case and the rotor fails earlier than expected. This is particularly important as the number of cycles
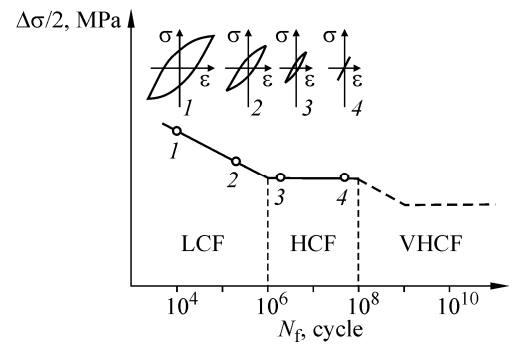
to failure is estimated for nominal stresses at which it is no greater than 10^5 flights.

Actually, the accumulation of damages for the low number of cycles to failure proceeds on the mesoscale, and its major mechanism in a disk is associated not with maximum stresses but with a combination of its maximum load and blade vibrations [15], which is most evident in Ti alloys [16].

The foregoing suggests that explaining the nature of very high cycle fatigue needs a more detailed analysis based on the scale hierarchy and synergetic principles of physical mesomechanics [17]. It is this issue that we consider below.

2. BIFURCATION REGION $(\Delta q_\sigma)_3$

In synergetic terms, any loaded metal in its continuous energy exchange with surroundings changes the leading mechanism of its evolution on approaching a certain critical level of damage accumulation. The mechanism that leads on one scale cannot lead on the others because each scale comes with a new mechanism of damage accumulation. Therefore, the fatigue of metals develops through cascade of changes of scales and mechanisms of fracture.

Each scale-to-scale transition represents a bifurcation region $(\Delta q_\sigma)_i$ with a certain interval of strain energy density or equivalent stress at which either of two respective mechanisms of damage accumulation is possible with a certain probability (Fig. 3).

The width of each bifurcation region and its position relative to stresses depends on many factors [18]. For example, the transition from low cycle fatigue to repeated static fracture with subsurface nuclei, like in monotonic tension, falls on the so narrow stress interval that on the macroscale it can confidently be taken as a single stress level $(\sigma_e)_0$. At this stress level, there are two ways of energy absorption, and hence, two
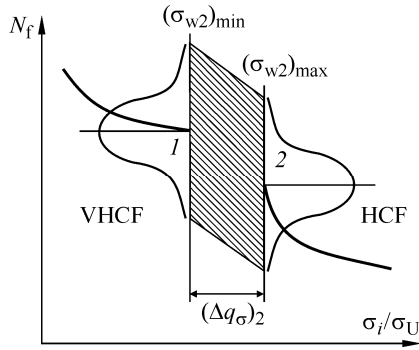
Fig. 3. Example of bimodal life distributions in bifurcation regions $(\Delta q_\sigma)_i$ where either of two curves with different exponents m (Eq. (2)) is possible with certain probability P_i. Transition region $(\Delta q_\sigma)_2$ is from very high to high cycle fatigue.

ways of crack nucleation are equiprobable: either surface or subsurface. It is the stress level at which the dependence $N_f = f(\sigma_e)$ changes its form.

The bifurcation diagram in Fig. 1 suggests that the transition boundary between the mesoscale (high cycle fatigue) and the macroscale (low cycle fatigue) is the state of a metal changing its behavior from macroscopically elastic to macroscopically plastic. Such an interpretation is clear from the diagram in Fig. 2, though we are dealing not with a certain stress corresponding to fatigue limit but with a certain stress range $(\Delta q_\sigma)_3$ showing the scatter of properties from specimen to specimen.

From our analysis it follows that the region $(\Delta q_\sigma)_3$ should include the threshold stress indicated in Fig. 2 but the stress variation should remain. Even in low cycle fatigue alone, the data scatter for metals is significant.

In fact, the Mughrabi diagram with one stress level for fatigue limit σ_{-1} suggests three failure mechanisms: low cycle fatigue with residual strains at about 10^6 cycles, high cycle fatigue with no hysteresis at about 10^7 cycles, and failure with no hysteresis at the transition to very high cycle fatigue at about 10^8 cycles. The existence of three failure scales with three different mechanisms of crack nucleation at one stress level is evidence for a multimodal life distribution in which each scale is probable.

Unlike the fatigue limit in the Mughrabi diagram, the region $(\Delta q_\sigma)_3$ is a bifurcation in which the life distribution can be only bimodal, with both characteristics lying near the yield strength of a material.

The change in the behavior of a metal in the region $(\Delta q_\sigma)_3$, originally described as a fatigue curve discontinuity [19], means that the metal near its yield

strength $\sigma_{0.2}$ is brought to an unstable state in which residual strains at the same stress level may or may not occur with a certain probability. Depending on the material type, three situations are possible in the region $(\Delta q_\sigma)_3$ [20]: low cycle fatigue with a shift toward longer lives compared to high cycle fatigue, low cycle fatigue with a shift toward shorter lives compared to high cycle fatigue, and low cycle fatigue with no shift but with its curve $N_f = f(\sigma_e)$ sloping differently than the curve of high cycle fatigue.

The state of a material in the region $(\Delta q_\sigma)_3$ depends largely on its ratio $\sigma_{0.2}/\sigma_U$. For example, for a metal with $0.71 < \sigma_{0.2}/\sigma_U < 0.83$, its behavior in different specimens can be both hardening and softening [21]. Hence, in the region $(\Delta q_\sigma)_3$, different specimens at the same stress level can show both hardening and softening effects, and this leads to two fatigue curves corresponding to their bimodal life distribution.

The width of the region $(\Delta q_\sigma)_3$ depends on the scatter of material characteristics and primarily of yield strength. For example, fatigue tests of low-carbon steel (0.16% C) with average grain sizes varied from specimen to specimen [22] show that increasing the grain size decreases the upper and lower yield strengths and the fatigue limit. It should be noted that with increase in grain size it also decreases the difference between the yield strength and fatigue limit, which influences the ratio $\sigma_{-1}/\sigma_{0.2}$. Similar results for low-carbon steel are reported elsewhere [23]. Increasing the average grain size decreases the lower yield strength $\sigma_{0.2}$ and the fatigue limit σ_{-1}, and at an aver-
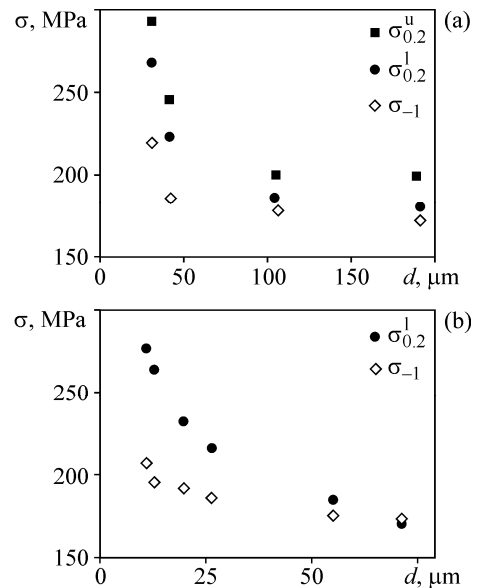

Fig. 4. Yield strength and fatigue limit versus grain size in low-carbon steel according to [22] (a) and [23] (b).

age grain size $d \approx 72$ μm, the fatigue limit exceeds the lower yield strength (Fig. 4).

Therefore, with statistically different average grain sizes, the fatigue life and the width of the region $(\Delta q_\sigma)_3$ can have a large scatter.

Thus, the region of bimodal life distribution $(\Delta q_\sigma)_3$ is fundamentally different from the transition region between very high and low cycle fatigue interpreted as fatigue limit and characterized by a multimodal life distribution.

Let us compare the bimodal and the multimodal life distribution at the transition from very high to high cycle fatigue [24].

3. MULTIMODAL LIFE DISTRIBUTION

In the very high cycle fatigue regime, the nucleation of subsurface cracks is due to different stress concentrators [3–8]. Moreover, one of its mechanisms involves the transition of a metal to a superplastic state in a fracture nucleus with the formation of mostly spherical nanostructures bordered by a fine granular area. Thus, in one and the same material, different sources can initiate subsurface fracture at the same stress whose level is much lower than the threshold σ_{w2}, or fatigue limit σ_{-1}, separating the meso- and microscales.

For example, as has been shown [25, 26], VT3-1 titanium specimens cut out of the compressor disk of an aircraft engine made to standards and operated trouble free for 8000 h have their fracture nuclei at the boundaries of a lamellar structure, its oriented regions, and cleavage facets of α-phase globules.

In a metal with high bulk anisotropy, different fracture nuclei at the same stress are possible with one or another probability, resulting in a multimodal life distribution and in a scatter of values by almost three orders of magnitude (10^8–10^{10} cycles) in the very high cycle fatigue regime.

Increasing the stress to $(\Delta q_\sigma)_2$, i.e., to the transition from very high to high cycle fatigue, shifts the site of fatigue crack nucleation to the surface layer of a metal such that the process begins to depend heavily on the nature and geometry of the surface whose high sensitivity to stress concentration provides a bimodal life distribution in the high cycle fatigue regime.

According to physical mesomechanics research, the concentration of surface stress in a metal is associated with its lattice curvature as a trigger for dislocation accumulation [27] and with a chessboard relief formed on its surface [28]. This brings inhomogeneity in the distribution of chemical elements and residual strains throughout the surface layer, including a thin upper oxide layer in contact with air. Air accelerates the motion of dislocations inward a material and shortens the time to their critical density and band structure formation which precedes crack nucleation in high cycle fatigue [20].

All these factors provide surface activation under increasing stress, and because several mechanisms in and on the surface of materials create conditions for crack nucleation, the region $(\Delta q_\sigma)_2$ shows a multimodal life distribution. One mode still serves for subsurface crack nucleation but with a lower probability at higher stresses, and the other two persist with different probabilities on the mesoscale up to a certain stress, whose level is yet to be analyzed to correlate it with mechanical characteristics of materials.

The fact of bimodal life distribution in high cycle fatigue was first identified and studied in metal materials based on Ni, Ti, Al, and Fe [29]. According to the study, the fatigue life scatter in the high cycle regime and near the region $(\Delta q_\sigma)_2$ fits the condition

$$\lg N_\Sigma = p_1 \lg N_1 + p_2 \lg N_2, \qquad (3)$$

where p_1, p_2 are the probabilities of two fracture mechanisms, and $\lg N_1$, $\lg N_2$ are the respective fatigue lives.

Note that similar experimental data are reported in many studies but without their analysis in the way suggested [29]. For example, in the standard that establishes the methods of fatigue tests of metals and
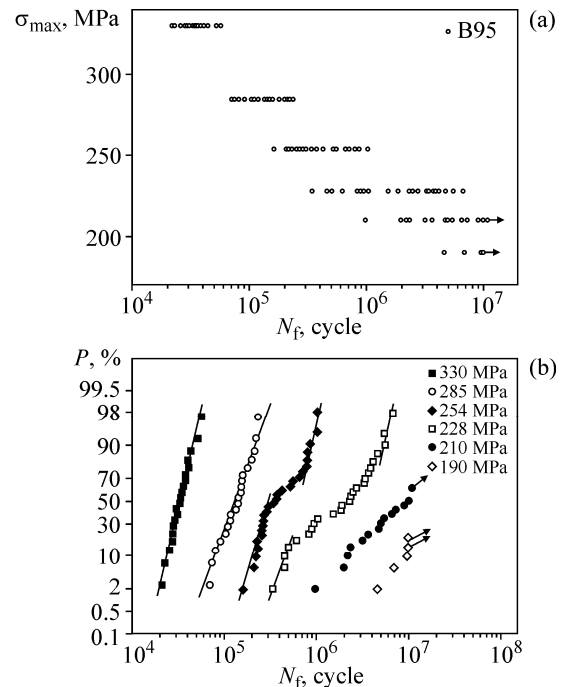

Fig. 5. Fatigue test data (a) and life distributions for B95 Al alloy specimens (b) according to [2].
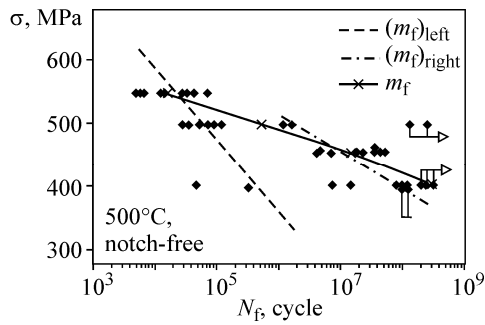
Fig. 6. Fatigue curves of smooth round VT9 Ti alloy specimens tested at 500°C: dashed and dash-dot lines for left and right branches of bimodal life distribution, solid line for averaged data.

Fig. 7. Fatigue nuclei (arrows) in smooth VT9 Ti alloy specimens after failure in rotating bending at about 10^7 (a) and 10^8 cycles (b).

alloys (RF GOST 25.502-79 [2]), experimental data are tabulated for B95 aluminum alloy subjected to up to 10^7 cycles of rotating cantilever bending at six stress levels, with 20 to 26 specimens tested at each stress. As can be seen from Fig. 5a, showing these data in graphic form, the life scatter at about 228 MPa is almost 10^5 to 10^7 cycles.

From probability curves of fatigue life in Fig. 5b, plotted for different stresses according to Weibull, it follows that not one but two life distributions with a transition region appear beginning with 254 MPa. This experimental fact suggests that more statistical data are needed to identify the bimodal life distribution on the mesoscale in the region $(\Delta q_\sigma)_2$. With a small number of specimens, the difference in the behavior of a metal is averaged and cannot be analyzed.

Figure 6 demonstrates the fatigue data of VT9 titanium alloy tested in air at 500°C [22] from which we can analyze the formation of fracture nuclei corresponding to two branches of its bimodal life distribution.

In both cases, we have crack nucleation from surface stress concentrators in the form of machining marks (Fig. 7). The bimodal life distribution suggests seemingly the same situation but the actual sources of cracks are different: physical stress concentration in a brittle surface layer at low stress and geometric stress concentration in machining marks at high stress.

Thus, two stages of mesoscale fracture are realized in a material under cyclic load. They can be termed meso I and meso II by analogy with the scale hierarchy of plastic deformation under monotonic tension [10]. On the meso I scale under increasing stress, we have a bimodal life distribution in which the dominant role belongs to physical stress concentration in a thin surface layer with four factors responsible for its critical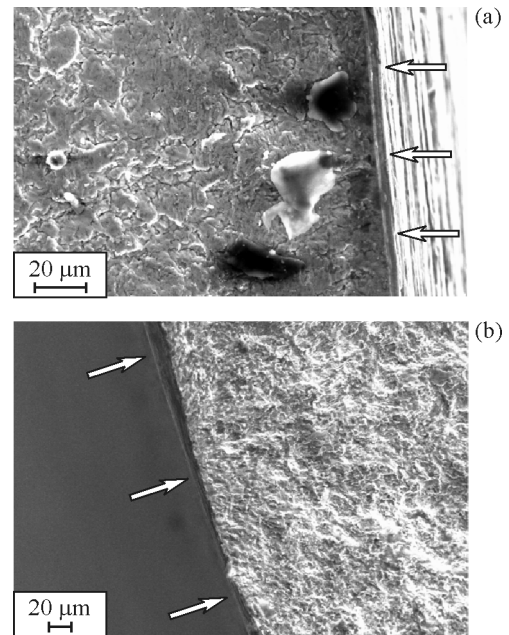 damage level: chemical inhomogeneity, residual stress, oxidation embrittlement, and lattice curvature as a driver of critical dislocation accumulation and band structure formation.

On the meso II scale under increasing stress, geometric stress concentration comes into play such that responsible for critical damage accumulation become geometric features, chessboard relief formation, and deformation vortices.

Hence, the mesoscale mechanisms of crack nucleation in high cycle fatigue are fundamentally different from the well-known macroscale mechanisms of banding which operate in low cycle fatigue and involve, according to physical mesomechanics, rotations of material volumes up to the point of knife boundary formation [10].

In the light of the foregoing, the complete diagram of metal fatigue is represented by three scales whose boundaries $(\Delta q_\sigma)_i$ feature bimodal and multimodal life distributions (Fig. 8). The fatigue limit of metals determined by available test methods is, in fact, a certain of the stress levels in the transition region $(\Delta q_\sigma)_i$. What is important is that only on the interval 3×10^6–10^8 cycles the quantity σ_{-1} can be taken as a fatigue limit. For each metal, the characteristic σ_{-1} is single but can fall on different scale transition regions $(\Delta q_\sigma)_i$ depending on the material type.

Let us compare the scale boundaries of metal fatigue and the fatigue limit σ_{-1} depending on the mechanical characteristics of a material.
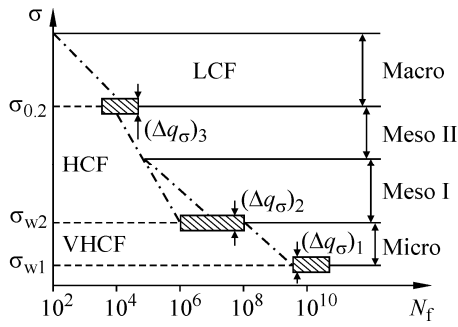
Fig. 8. Complete diagram of metal fatigue, according to Wöhler concept, in terms of three scales of damage accumulation, bifurcation regions $(\Delta q_\sigma)_i$, and bimodal life distribution on mesoscale.

4. SCALE BOUNDARIES

Our analysis shows that the fatigue limit of materials as a behavioral characteristic represents the upper boundary of transitions between different scales. In fact, the limiting state of a material means a change of damage accumulation scales in a crack nucleation zone. The value of σ_{-1} can be determined reasoning from mechanical characteristics [30]. In view that the width of one of the transition zones $(\Delta q_\sigma)_3$ from high to low cycle fatigue depends on the ratio $\sigma_{0.2}/\sigma_U$, we have analyzed how the fatigue limit σ_{-1} is influenced by the mechanical characteristics $\sigma_{0.2}$ and σ_U and the ratio $\sigma_{-1}/\sigma_{0.2}$ by $\sigma_{0.2}/\sigma_U$ in about 250 aircraft structural materials based on Fe, Al, Mg, Ti, and Cu [31].

The analysis shows that the fatigue limit σ_{-1} responds to variations in $\sigma_{0.2}$ and σ_U in the same way: it increases with both (Fig. 9). At the same time, the scatter of σ_{-1} for some materials grows, i.e., its dependence on $\sigma_{0.2}$ and σ_U is weakened. This is because different metals behave differently under cyclic loading. For steels, for example, the scatter of σ_{-1} in relation to $\sigma_{0.2}$ or σ_U increases slightly, while its increase for Ti alloys is much more pronounced.

According to quantitative estimates, $\sigma_{-1} = A\sigma_{0.2}^\alpha$ or $\sigma_{-1} = B\sigma_{0.2}^\beta$, where A and B are some constants, α and β are the exponents, which does not contradict the dependences obtained earlier [30].

For Cu-based aircraft materials, the values of the constants and exponents are $A = 7.88$, $B = 1.44$, $\alpha = 0.51$, $\beta = 0.75$, and for Fe- and Al-based ones, they are $A = 6.52$, $\alpha = 0.63$ and $B = 0.66$, $\beta = 0.86$, respectively. For Ti- and Mg-based materials, the fatigue limit is scattered widely in relation either to their yield strength or to their ultimate strength, and any functional dependence between these characteristics fails.
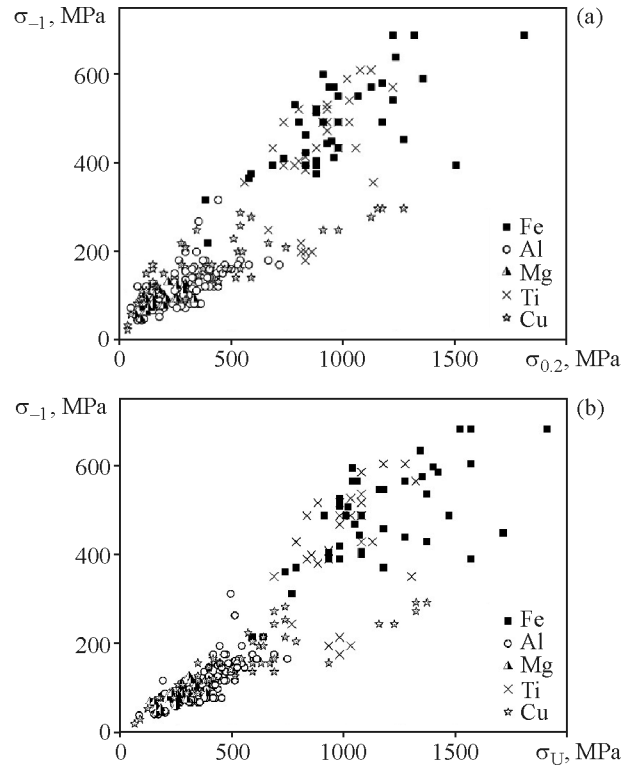

Fig. 9. Fatigue limit versus yield strength (a) and ultimate strength (b) according to reference data for aircraft materials based on Fe, Al, Mg, Ti, and Cu [31].

In the dependence of $\sigma_{-1}/\sigma_{0.2}$ on $\sigma_{0.2}/\sigma_U$, the boundary determined by the fatigue limit σ_{-1} characterizes the transition from very high to high cycle fatigue if $\sigma_{-1}/\sigma_{0.2} < 1$ and from very high to low cycle fatigue if $\sigma_{-1}/\sigma_{0.2} \geq 1$. Our comparative analysis of the ratios $\sigma_{-1}/\sigma_{0.2}$ and $\sigma_{0.2}/\sigma_U$ shows that almost all among the aircraft structural materials considered fit the condition $\sigma_{-1}/\sigma_{0.2} < 1$, except only for six Cu-based alloys, three Al-based alloys, and one Mg-based alloy where $\sigma_{-1}/\sigma_{0.2} \geq 1$ (Fig. 10). Hence, the high cycle fatigue
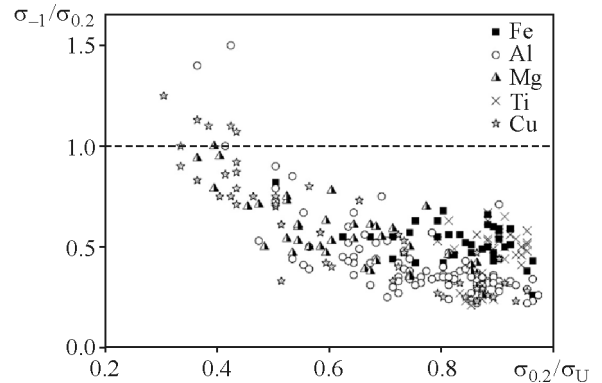

Fig. 10. Ratio $\sigma_{-1}/\sigma_{0.2}$ versus ratio $\sigma_{0.2}/\sigma_U$, according to reference data for aircraft materials based on Fe, Al, Mg, Ti, and Cu [31].
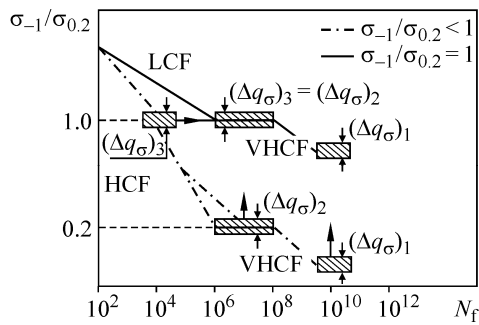
Fig. 11. Diagram of metal fatigue with bifurcation regions $(\Delta q_\sigma)_i$ plotted according to Wöhler concept for $\sigma_{-1}/\sigma_{0.2} = 1$ (case considered by Mughrabi) and for $\sigma_{-1}/\sigma_{0.2} < 1$ (general case).

regime is the main range for aircraft materials operating under cyclic loads without residual plastic strains.

From the comparative data on $\sigma_{-1}/\sigma_{0.2}$, and $\sigma_{0.2}/\sigma_U$, and in view of all fracture scales corresponding to very high, high, and low cycle fatigue (Fig. 8), we can suggest the following general regularity in the cyclic load response of materials differing in mechanical characteristics (Fig. 11). As the ratio $\sigma_{-1}/\sigma_{0.2}$ increases, the regions $(\Delta q_\sigma)_1$ and $(\Delta q_\sigma)_2$ shift upward (Fig. 11, up arrows) and decrease the stress regime for the mesoscale with high cycle fatigue. Simultaneously, the region $(\Delta q_\sigma)_3$ shifts to the range of higher fatigue lives (Fig. 11, rightward arrow) such that the maximum number of cycles for low cycle fatigue approaches 10^6 in the limit. The boundary of low cycle fatigue in terms of durability corresponds to a minimum value of about 10^4 cycles at minimum $\sigma_{-1}/\sigma_{0.2}$ which is about 0.2 in the aircraft materials studied. Hence, the boundary of maximum durability in the low cycle fatigue regime is determined by the ratio $\sigma_{-1}/\sigma_{0.2}$ rather than by the mechanical characteristics.

5. CONCLUSION

The so-called fatigue limit is, in fact, the upper boundary of the stress interval $(\Delta q_\sigma)_i$ with a multimodal life distribution. At $\sigma_{-1}/\sigma_{0.2} < 1$, the interval $(\Delta q_\sigma)_i$ corresponds to the transition from very high cycle fatigue (micro- or nanoscale) to high cycle fatigue (mesoscale), and at $\sigma_{-1}/\sigma_{0.2} \geq 1$, to the transition from very high to low cycle fatigue (macroscale). As the ratio $\sigma_{0.2}/\sigma_U$ decreases, the ratio $\sigma_{-1}/\sigma_{0.2}$ in aircraft materials tends to increase up to unity such that the mesoscale or the high cycle fatigue regime degenerates.

The transition to the mesoscale features a bimodal life distribution with successive changes in the proba-

bility of two mechanisms of crack nucleation dominating respectively on two scales: meso I and meso II.

On the meso I scale, the factors responsible for critical damage accumulation in the surface layer of materials include its chemical inhomogeneity, residual stress, oxidation embrittlement, and lattice curvature as a driver for critical dislocation accumulation and band structure formation.

On the meso II scale, they include geometric stress concentrators, chessboard relief formation, and deformation vortices.

On the macroscale, the nucleation of fracture in metals is associated with intense sliding and rotations of material volumes up to the point of knife boundary formation.

REFERENCES

1. *Machine Building, Encyclopedia, Vol. II-1: Physico-Mechanical Properties. Testing of Metallic Materials*, Mamaeva, E.I, Ed., Moscow: Mashinostroenie, 2010.

2. RF GOST 25.502-79: *Strength Analysis and Testing in Machine Building. Methods of Metals Mechanical Testing. Methods of Fatigue Testing*, 2005.

3. Bathias, C. and Paris, P.C., *Gigacycle Fatigue in Mechanical Practice*, New York: Marcel Dekker, 2005.

4. *Proceedings of the III International Conference on Very High Cycle Fatigue (VHCF-3), September 16–19, 2004, Ritsumeikan University, Kusatsu, Japan*, Sakai, T. and Ochi, Y., Eds., Japan: The Society of Materials Science, 2004.

5. *Proceedings of the VI International Conference on Very High Cycle Fatigue (VHCF-4), August 19–22, 2007, University of Michigan, Ann Arbor, Michigan, USA*, Allison, J.E., Jones, J.W., Larsen, J.M., and Ritchie, R.O., Eds., Ann Arbor: TMS, 2007.

6. *Proceedings of the VII International Conference on Very High Cycle Fatigue (VHCF-7), July 3–5, 2017, Dresden, Germany*, Zimmermann, M. and Christ, H.-J., Eds., Dresden: DVM, 2017.

7. Shanyavskiy, A., Ultrahigh Plasticity Behavior of Metallic Materials in the Ultra-High-Cycle (or Gigacycle, Very-High-Cycle) Fatigue Regime, *Key Eng. Mater.*, 2016, vol. 664, pp. 231–245.

8. Shanyavsky, A.A., Scales of Metal Fatigue Cracking, *Phys. Mesomech.*, 2015, vol. 18, no. 2, pp. 163–173.

9. Mughrabi, H., Specific Features and Mechanisms of Fatigue in the Ultrahigh-Cycle Regime, *Int. J. Fatigue*, 2006, vol. 28(11), pp. 1501–1508.

10. Panin, V.E., Overview on Mesomechanics of Plastic Deformation and Fracture of Solids, *Theor. Appl. Fract. Mech.*, 1998, vol. 30(1), pp. 1–11.

11. Palmgren, A.G., Die Lebensdauer von Kugellagern, *Zeitschrift des Vereines Deutscher Ingenieure* (*VDI Zeitschrift*), 1924, vol. 68, no. 14, pp. 339–341.

12. Miner, M.A., Cumulative Damage in Fatigue, *J. Appl. Mech. A*, 1945, pp. 159–164.

13. Shanyavsky, A.A., Safe Operation of First-Stage LPC Disks of D-30KU Engines by Fatigue Crack Growth Criteria, *Probl. Bezopasn. Polyot.*, 2011, no. 1, pp. 20–49.

14. Shanyavskiy, A.A., Fatigue Crack Propagation in Turbine Disks of EI698 Superalloy, *Frattura Integrità Strutturale*, 2013, vol. 7, no. 24, pp. 13–25.

15. Shanyavskiy A.A., *Safe Fatigue Failure of Aircraft Structures*, Ufa: Monograph, 2003.

16. Marci, G., Non-Propagation Conditions (ΔK_{th}) and Fatigue Crack Propagation Threshold (δK_T), *Fatigue Fract. Eng. Mater. Struct.*, 1994, vol. 17, no. 8, pp. 891–908.

17. Panin, V.E., Synergetic Principles of Physical Mesomechanics, *Phys. Mesomech.*, 2000, vol. 3, no. 6, pp. 5–34.

18. Shanyavsky, A.A., *Simulation of Fatigue Fracture of Metals. Synergetics in Aviation*, Ufa: Monograph, 2007.

19. Shabalin, V.I., Experimental Investigation of Fatigue Curve Shape, in *Strength of Metals under Cyclic Loading*, Ivanova, V.S., Ed., Moscow: Nauka, 1967, pp. 162–169.

20. Ivanova, V.S. and Terentiev, V.F., *Nature of Fatigue of Metals*, Moscow: Metallurgia, 1975.

21. Terentiev, V.F., General Fatigue Mechanisms in BCC Metals, in *Cyclic Fracture Toughness of Metals and Alloys*, Moscow: Nauka, 1981, pp. 45–52.

22. Yokobori, T., *An Interdisciplinary Approach to Fracture and Strength of Solids*, Groningen: Wolters-Noordhoff Scientific Publ., 1968.

23. Phillips, W.L. and Armstrong, R.W., The Influence of Specimen Size, Polycrystal Grain Size, and Yield Point Behaviour on the Fatigue Strength of Low-Carbon Steel, *J. Mech. Phys. Solids*, 1969, vol. 17, no. 4, pp. 265–270.

24. Shanyavskiy, A., Zaharova, T., and Potapenko, Yu., The Nature of Multi-Modal Distribution of Fatigue Durability for Titanium Alloy VT9, in *Proceedings of the Forth International Conference on Very High Cycle Fatigue (VHCF-4), August 19–22, 2007, University of Michigan, Ann Arbor, Michigan, USA*, Allison, J.E., Jones, J.W., Larsen, J.M., and Ritchie, R.O., Eds., TMS, 2007, pp. 325–330.

25. Nikitin, A., Palin-Luc, T., and Shanyavskiy, A., Crack Initiation in VHCF Regime on Forged Titanium Alloy under Tensile and Torsion Loading Modes, *Int. J. Fatigue*, 2016, vol. 93(2), pp. 318–325.

26. Nikitin, A., Palin-Luc, T., Shanyavskiy, A., and Bathias, C., Comparison of Crack Paths in a Forged and Extruded Aeronautical Titanium Alloy Loaded in Torsion in the Gigacycle Fatigue Regime, *Eng. Fract. Mech.*, 2016, vol. 167, pp. 259–272.

27. Panin, V.E., *Physical Mesomechanics of Materials* (in 2 vol.), Tomsk: TSU, 2015.

28. Panin, V.E., Panin, A.V., and Moiseenko, D.D., Physical Mesomechanics of a Deformed Solid as a Multilevel System. II. Chessboard-Like Mesoeffect of the Interface in Heterogeneous Media in External Fields, *Phys. Mesomech.*, 2007, vol. 10, no. 1–2, pp. 5–14.

29. Zakharova, T.P., On the Problem Concerned with the Statistical Nature of Fatigue Damage of Steels and Alloys, *Strength Mater.*, 1974, vol. 6, no. 4, pp. 415–421.

30. Troshchenko, V.T. and Sosnovsky, L.A., *Fatigue Resistance of Metals and Alloys*, *Handbook*, Kiev: Naukova Dumka, 1987, Part 1.

31. *Aircraft Materials*, *Handbook* (in 9 vol.), Tumanov, A.T., Ed., Moscow: VIAM, 1975.